Cell

Hydrodynamic Flow-Mediated Protein Sorting on the Cell Surface of Trypanosomes

Markus Engstler,[1,3,*] Thomas Pfohl,[2] Stephan Herminghaus,[2] Michael Boshart,[3] Geert Wiegertjes,[4] Niko Heddergott,[1] and Peter Overath[5]
[1]Institut für Mikrobiologie und Genetik, Technische Universität Darmstadt, Schnittspahnstrasse 10, 64287 Darmstadt, Germany
[2]Max-Planck-Institut für Dynamik und Selbstorganisation, Bunsenstrasse 10, 37073 Göttingen, Germany
[3]Department Biologie I, Genetik, Ludwig-Maximilians-Universität, Maria-Ward-Strasse 1a, 80638 München, Germany
[4]Cell Biology and Immunology Group, Wageningen Institute of Animal Sciences, Marijkeweg 40, 6709 PG, Wageningen, The Netherlands
[5]Interfakultäres Institut für Zellbiologie, Abteilung Immunologie, Universität Tübingen, Auf der Morgenstelle 15, 72076 Tübingen, Germany
*Correspondence: engstler@bio.tu-darmstadt.de
DOI 10.1016/j.cell.2007.08.046

SUMMARY

The unicellular parasite *Trypanosoma brucei* rapidly removes host-derived immunoglobulin (Ig) from its cell surface, which is dominated by a single type of glycosylphosphatidylinositol-anchored variant surface glycoprotein (VSG). We have determined the mechanism of antibody clearance and found that Ig-VSG immune complexes are passively sorted to the posterior cell pole, where they are endocytosed. The backward movement of immune complexes requires forward cellular motility but is independent of endocytosis and of actin function. We suggest that the hydrodynamic flow acting on swimming trypanosomes causes directional movement of Ig-VSG immune complexes in the plane of the plasma membrane, that is, immunoglobulins attached to VSG function as molecular sails. Protein sorting by hydrodynamic forces helps to protect trypanosomes against complement-mediated immune destruction in culture and possibly in infected mammals but likewise may be of functional significance at the surface of other cell types such as epithelial cells lining blood vessels.

INTRODUCTION

In the fluid mosaic model of Singer and Nicolson (1972), integral membrane proteins move by Brownian motion unless specific interactions lead to their aggregation. Sorting in the plane of the membrane involves specific protein-protein interactions, a classic example being the formation of the purple membrane composed of bacteriorhodopsin in Halobacteria, or complex formation with components on the inside or outside of the cell, such as the recruitment of receptors in clathrin-coated vesicles or the clustering of T cell receptors on CD4 cells in the contact area with B cells.

The possibility of molecular sorting on cell surfaces induced by the hydrodynamic shear force that acts on cells from flow of the external medium such as on cells in the mammalian circulation or on actively swimming unicellular organisms has, to our best knowledge, not been considered. However, the study of effects of shear stress on cells is an active field of investigation (see, for example, Fache et al., 2005; Phan et al., 2006; Tzima, 2006).

In this manuscript, we describe a sorting phenomenon on the surface of the unicellular hemoflagellate *Trypanosoma brucei*, which appears to use hydrodynamic flow force as part of its strategy for evasion from the mammalian humoral immune system. African trypanosomes cause persistent infections with a fluctuating parasitemia, which entails at least three different survival strategies. First and most important is antigenic variation of the surface coat (Cross, 1996). The trypanosome cell surface is covered with a monolayer of the variant surface glycoprotein (VSG) that acts as a physical barrier to the host immune system. Antigenic variation is centered on the exclusive expression of a single VSG gene and low-frequency, stochastic switching from expression of one VSG gene to another from a genomic repertoire of many hundreds. The newly expressed VSG is antigenically novel, and the cell proliferates until the host mounts a sufficient immune response (Barry and McCulloch, 2001). Second, immunosuppression results from a dramatic repression of stimulatory components by unknown mechanisms (Donelson et al., 1998). Third, clearance of surface-bound antibodies is effective at low to moderate antibody concentrations but is not sufficient to protect the cells at

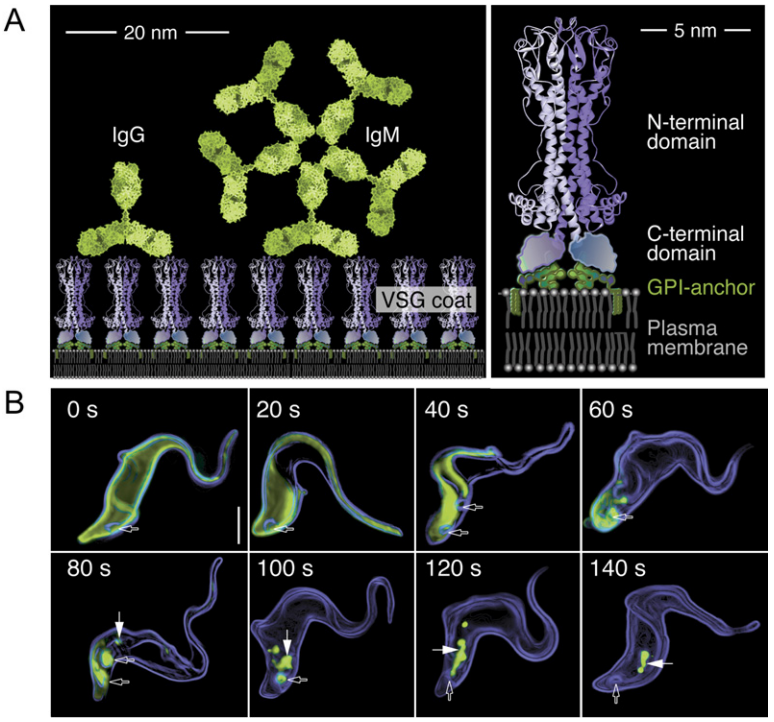

Figure 1. Host-Derived Antibodies Are Removed from the Cell Surface of Bloodstream Stage *Trypanosoma brucei*

(A) Schematic representation (drawn to scale) of IgG and IgM molecules bound to the trypanosome variant surface glycoprotein (VSG) coat (left). VSGs are homodimers (monomers in light blue and purple) that are attached to the plasma membrane via GPI anchors (right).

(B) Visualization of antibody removal. Cells were surface labeled with blue-fluorescent AMCA-sulfo-NHS and incubated at a density of 10^8 cells/ml for 10 min on ice with 0.1 mg/ml VSG-specific IgG, resulting in antibody labeling of 0.26% of all VSG dimers on the plasma membrane. Following 0-3 min of incubation at 37°C, cells were chemically fixed and permeabilized. Anti-VSG antibodies were detected with species-specific Alexa Fluor 488-conjugated second antibodies (green). Open arrows indicate the position of the flagellar pocket, and filled arrows point to the lysosome. Scale bar, 3 μm.

high antibody titers (McLintock et al., 1993). Antigenic variation and immunosuppression favor the long-term persistence of an infecting population, whereas clearance of surface-bound immunoglobulin may support the survival of individual cells during the emergence of a specific humoral immune response (Stevens and Moulton, 1978; Barry, 1979; Balber et al., 1979; Webster et al., 1990; Russo et al., 1993; O'Beirne et al., 1998), possibly favoring transmission by the insect vector. The experiments presented in this study suggest an unusual mechanism for the clearance of antibodies from the surface of the parasite.

RESULTS

Antibody-VSG Complexes Are Sorted on the Cell Surface Prior to Localized Endocytosis

Antibodies that recognize VSG can bind over the entire trypanosome cell surface but can only be endocytosed through the flagellar pocket, the sole site for endocytosis and membrane recycling (Engstler et al., 2004; Overath and Engstler, 2004). To visualize this process in live cells, cell-surface VSG (Figure 1A) was labeled with a membrane-impermeable blue-fluorescent dye; the cells were then exposed to VSG-specific immunoglobulin G (IgG) antibodies such that ~1 in 400 VSG dimers formed an IgG-VSG complex. Both the VSG labeling and antibody binding were performed at 0°C, and at this temperature, there was no endocytosis of the VSG or IgG, and all IgG-VSG remained on the cell surface. The cells were then warmed to 37°C, and the location of the IgG was determined over a time course by immunofluorescence microscopy (Figure 1B). Initially (0 s), IgG-VSG homogenously covered the cell body and flagellum but was not detectable in the flagellar pocket. Upon warming to 37°C, the antibodies entered the flagellar pocket (Figure 1B). Remarkably, the clearance of IgG-VSG from the cell surface was directional, and within 30–60 s all IgG-VSG had been sorted to the posterior end of the cell, where there was transient accumulation before uptake by endocytosis via the flagellar pocket (Figure 1B; 80–120 s) and transport to the lysosome (Figure 1B; 140 s). The individual steps of IgG-VSG removal, namely movement to the posterior end, entry into the flagellar pocket, and endocytosis, are characterized by distinct temperature dependencies (Figure 2). IgG-VSG accumulated at the posterior pole at temperatures between 12°C and 37°C, while access to the flagellar pocket and endocytosis were slowed down at 24°C and were essentially halted at lower temperatures.

The intracellular fate of the IgG and VSG was determined using 3D fluorescence microscopy and quantitative colocalization analyses with organelle-specific marker proteins. The majority of IgG was transported to the lysosome, where the IgG was degraded (O'Beirne et al., 1998; Pal et al., 2003), whereas the VSG was recycled to the cell surface (Figure S1). Thus, the directional movement of cell surface IgG-VSG toward the posterior end of the cell and the subsequent rapid endocytosis (Engstler et al., 2004) provides a very efficient mechanism to clear immune complexes from the cell surface.

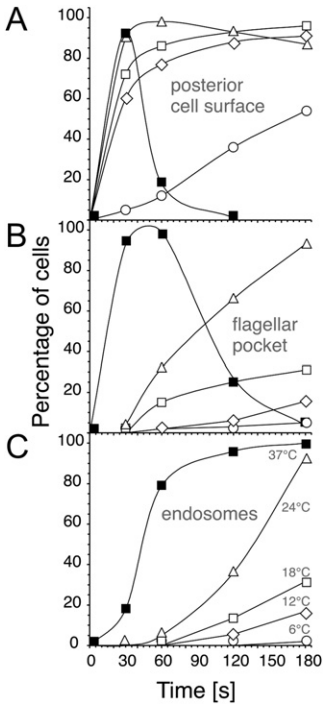

Figure 2. The Removal of Antibodies from the Trypanosome Cell Surface Is a Three-Step Process that Is Characterized by Distinct Temperature Sensitivities

(A) Rapid accumulation of IgG-VSG at the posterior pole of trypanosomes occurs at temperatures ranging from 12°C to 37°C.

(B) While at 37°C IgG-VSG gains access to the flagellar pocket, the entry into this compartment is delayed or impeded at lower temperatures.

(C) Endocytosis of IgG-VSG reveals a similar temperature sensitivity as the entry into the flagellar pocket. Black squares, 37°C; white triangles, 24°C; white squares, 18°C; white diamonds, 12°C; white circles, 6°C.

Rapid Antibody Clearance Protects Bloodstream Stage Trypanosomes from Complement-Mediated Lysis

The single-cell experiments suggested that the removal of IgG-VSG from the trypanosome surface is much faster than previously described (Russo et al., 1993). Flow cytometry was used to analyze IgG-VSG clearance in a population, and the half-times measured were similar to those obtained in single-cell experiments: 35 s for a polyvalent anti-VSG IgG and 43 s for a monoclonal IgG (Table 1). The experiments above were performed with proliferating trypanosomes, which have a slender morphology. The analysis was repeated with trypanosomes with a "stumpy" morphology, which have arrested in G1 of the cell cycle, a natural response to high cell density. A predominantly stumpy population cleared IgG-VSG from the cell surface with a half-life of 20 s, about twice as fast as determined for slender trypanosomes (Table 1). Although the rate of directional movement of IgG-VSG toward the posterior end of the cell was similar in both cell types, the stumpy trypanosomes showed little or no posterior accumulation of antibody complexes. The

Table 1. Kinetics of Cell Surface Clearance of VSG-Bound Ligands

Ligand	Half-Life of Cell Surface Fluorescence (s)	Posterior Accumulation of Surface Fluorescence
Polyclonal IgG		
Monomorphic	35.3 ± 4.6	+
Pleomorphic, slender	36.2 ± 1.8	+
Pleomorphic, stumpy	19.7 ± 2.1	–[a]
Monoclonal IgG	42.9 ± 4.6	+
$F(ab')_2$	167.1 ± 19.8	–
Fab	193.6 ± 15.7	–
TAC	18.3 ± 1.3	+
TAC + dextran	17.0 ± 2.4	+
IgM	13.4 ± 3.2	+
Streptavidin	168.1 ± 6.8	–

If not otherwise stated, all experiments were done with monomorphic bloodstream stage *T. brucei*. The percentage of surface VSG labeling was 1% for all ligands. The rates were calculated from graphs shown in Figure S2.

[a] No posterior accumulation of IgG was observed, corresponding to the faster endocytic uptake in stumpy stage cells compared to slender cells.

simplest explanation for the lack of posterior accumulation in stumpy cells is that the endocytic rate is higher and is sufficient to remove IgG-VSG as it arrives at the posterior pole. This model is consistent with the larger flagellar pocket and higher rate of endocytosis observed in stumpy forms (Engstler et al., 2004; and data not shown).

The next experiment tested whether the rapid clearance of IgG-VSG from the cell surface was protective against antibody-mediated complement lysis. Trypanosomes were incubated with varying concentrations of anti-VSG IgG on ice and warmed to 37°C, and then complement was added over a time course and cell viability was assayed 25 min after complement addition (Figure 3A). The results demonstrated that preincubation at 37°C before complement addition rendered the IgG-loaded cells resistant to complement. Even at the highest IgG concentrations tested, incubation for 10 min at 37°C was sufficient to make the trypanosomes fully resistant to antibody-mediated complement action. The length of incubation at 37°C required to protect the cells was inversely related to the amount of IgG loaded onto the cells (Figure 3A). Therefore, up to a certain antibody concentration, surface clearance of IgG-VSG provides a means to escape complement-mediated lysis. The same assay was used to compare the degree of protection against complement in stumpy and slender cells. The stumpy cells became resistant to complement more rapidly than slender cells, consistent with their higher rate of endocytosis

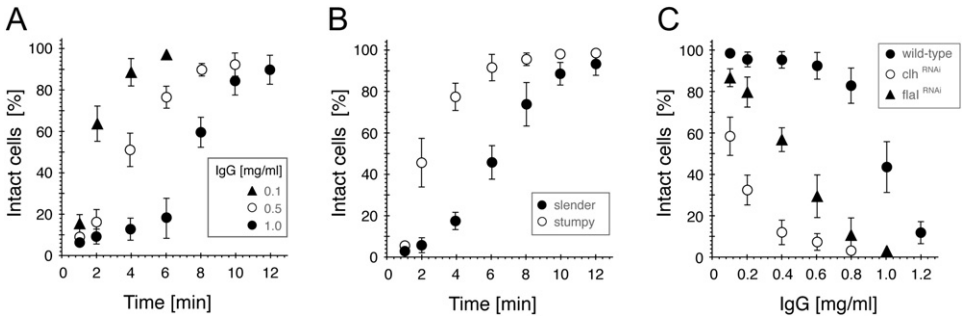

Figure 3. The Removal of Antibodies from the Cell Surface Renders *T. brucei* Resistant to Complement-Mediated Lysis

Semiautomated analysis of complement-mediated lysis of bloodstream stage trypanosomes was carried out by fluorescence threshold segmentation of microscopic images. Live cells were fluorescently stained at the surface with AMCA-sulfo-NHS. This blue-fluorescent dye specifically labels cell surface protein of living cells. In dying or dead cells the compound has access to the cytosol, resulting in a bright blue fluorescence of the entire cell body. Images with 20 to 30 trypanosomes each were segmented using the edge criterion, which is based on the intensity properties of the structure. The result was a masked image with two distinct groups of objects (living and dead cells), which were automatically scored and counted by an IPLab software script.

(A) The acquisition of resistance to guinea pig complement depends on the concentration of anti-VSG IgG (0.1, 0.5, and 1 mg/ml; corresponding to fractional VSG labeling of 0.26%, 2.6%, and 9.2%, respectively).

(B) Cell cycle-arrested stumpy stage trypanosomes remove VSG-antibody complexes faster than proliferating slender stage cells (0.8 mg/ml; percentage of VSG molecules labeled: stumpy cells, 3.3%; slender cells, 3.1%).

(C) Directional cellular motility and endocytosis both are required for complement resistance. Complement resistance is shown as a function of antibody concentration for wild-type cells and cells where either the clathrin heavy chain (CLH) or the Fla1 protein has been downregulated by RNAi. Values are means ± SEM (n = 4).

(Figure 3B; McLintock et al., 1993). All experiments used a batch process of antibody binding and clearance to facilitate measurements of half-lives.

Sorting of Antibody-VSG Complexes on the Cell Surface Is Independent of Endocytosis but Requires Cellular Motility

What causes the rapid movement of IgG-VSG to the posterior end of the cells? First, the process is active, as the directional movement toward the posterior was reduced by increasing concentrations of the metabolic inhibitor 2-deoxyglucose and was absent in energy-depleted, immotile cells, which remained uniformly coated with IgG (data not shown). Second, the accumulation of IgG-VSG at the posterior end is independent of endocytosis. RNAi-mediated knockdown of clathrin heavy chain causes a block of all endocytic traffic and an increase in the size of the flagellar pocket due to ongoing exocytosis (Allen et al., 2003; Overath and Engstler, 2004). In clathrin-depleted cells, IgG-VSG still concentrated at the posterior of the cell near the flagellar pocket with the same kinetics as control cells but was not internalized (Figures 4A and 4B, middle panels). A block of plasma membrane recycling was previously demonstrated in trypanosomes depleted of actin by RNAi (Garcia-Salcedo et al., 2004). While blocking endocytic traffic, the absence of actin had an effect neither on the movement of IgG-VSG to the posterior pole of the trypanosome (Figure 5A) nor on the motility of the cell. Because redistribution of immune complexes was independent of endocytosis and actin, a force must be applied outside the cell. Therefore, we tested the hypothesis that the force causing IgG-VSG directional movement originates from cell motility.

When placed in serum, *T. brucei* cells swim continuously with an average speed of 20 $\mu m\ s^{-1}$ with a directional, drill-like motion. The directional swimming is dependent on the single flagellum, which emerges from the flagellar pocket, is attached to the cell body, and extends beyond the anterior pole of the cell. Thus, the flagellum points in the direction of movement, and the flagellar pocket is located at the posterior end of the cell body. Trypanosome movement in standard culture medium containing 10% serum is deceptive. Culture medium is not as viscous as blood, the natural milieu, and at any one time one-third of all cells were swimming, but two-thirds tumbled. In culture media, the fraction of cells showing directional movement of cell surface IgG-VSG was 44%. In fluids of higher viscosity, such as undiluted serum, or in the presence of obstacles, such as blood cells, up to 90% of trypanosomes swam directionally, and all showed posterior IgG-VSG accumulation (Table S1).

Inducible RNAi-mediated knockdown of the FLA1 gene was used to ablate trypanosome swimming (LaCount et al., 2002), and the effect on the directional movement of IgG-VSG was determined (Figure 4). The FLA1 protein is essential for connecting the flagellum to the cell body, and its downregulation by RNAi results in detachment of the flagellum and loss of directional cell motility (LaCount et al., 2002). In the noninduced control cells, about 80% of the IgG-VSG accumulated at the posterior fifth of the cell surface within 0.5 min (Figure 4A, upper panel). Within 3 min all IgG-VSG disappeared from the posterior end and was then located in the lysosome (Figure 4B, upper panel).

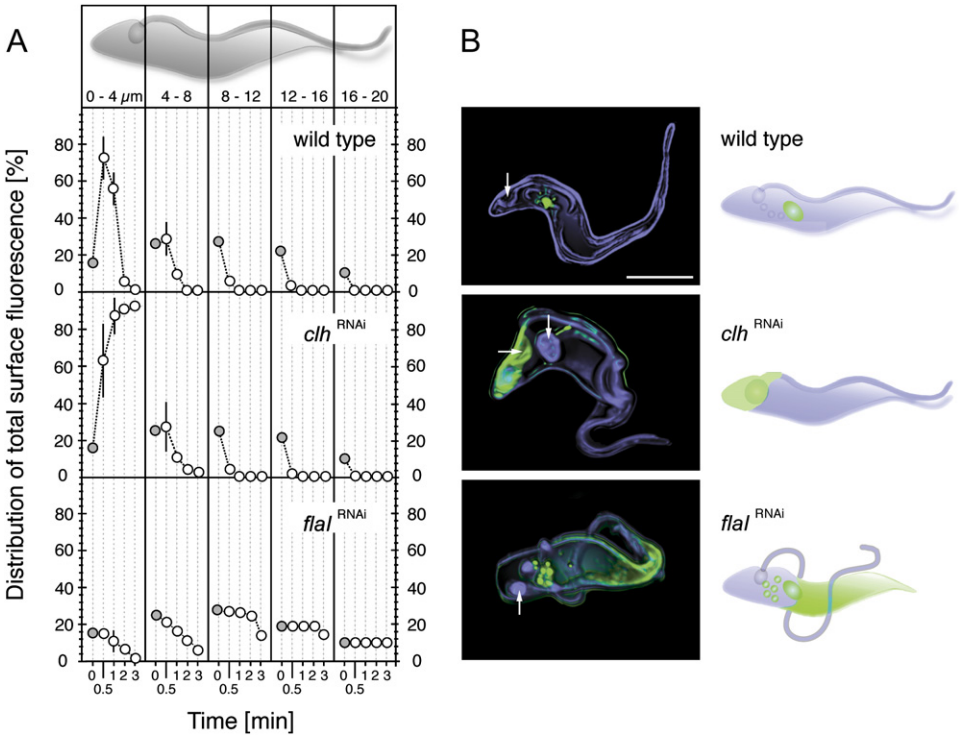

Figure 4. The Removal of Antibodies from the Trypanosome Cell Surface Requires Endocytosis and Cellular Motility

Trypanosomes were cell surface labeled with AMCA-sulfo-NHS and treated with anti-VSG antibodies. The time-dependent changes in the localization of surface-bound antibodies were measured by sectioning two-channel, deconvolved 3D images of cells (z-dimension 60 × 150 nm). The major axis (x) through the cell body was automatically defined by measuring the eccentricity of the object using the IPLab software. For analysis only those cells were chosen that were oriented in the optical plane. Along the x axis the cell surface was divided into consecutive 4 μm segments, and the fluorescence intensity of each segment was measured and compared to the total cell surface fluorescence.

(A) Quantification of the distribution of anti-VSG antibodies on the cell surface of wild-type and transgenic bloodstream stage *T. brucei*. Cells were treated as described for Figure 1B. Deconvolved 3D images were automatically scored for eccentricity and aligned for digital segmentation along the x axis. The distribution of IgG visualized by fluorescent secondary antibodies was measured on five consecutive surface segments along the longitudinal cell x axis using the blue AMCA fluorescence as a marker for the plasma membrane. Values are given as percentage of total antibody fluorescence and are means ± SEM of 12 measurements.

(B) Cells were treated as in (A), incubated at 37°C for 3 min, fixed, and permeabilized. Images on the left are maximum-intensity projections of representative, deconvolved two-channel 3D data sets. Linear false coloring of grayscale images was done prior to merging of the two image channels. Arrows indicate the flagellar pocket. The schematic drawings (right) illustrate the typical distribution of anti-VSG antibodies (green). Scale bar, 5 μm.

In FLA1-depleted trypanosomes, IgG-VSG did not accumulate at the posterior of the cell, but the area around the flagellar pocket was depleted of IgG-VSG (Figures 4A and 4B, lower panels). This observation can be explained if endocytosis and subsequent IgG degradation in the lysosome proceeded after entry into the flagellar pocket by diffusion in the absence of motility.

The effect of the RNAi knockdowns of clathrin and FLA1 on the sensitivity to complement-mediated lysis was tested (Figure 3C). Wild-type trypanosomes were significantly more resistant than cells depleted of either clathrin heavy chain or FLA1. The clathrin-depleted cells, in which all the IgG-VSG remained on the cell surface, were more readily killed by complement than the immotile, FLA1-depleted cells, which have a reduced rate of internalization of IgG-VSG.

The experiments above indicated that the direction of cellular motility influences the movement of IgG-VSG. This assumption was experimentally tested using trypanosomes with the direction of movement reversed following depletion of the dynein arm intermediate chain, which leads to reversal of flagellar beat (Branche et al., 2006). As a result of this reversal the cells swim backward. Strikingly, in these cells, IgG-VSG accumulated at the anterior pole of the cell and was absent from the posterior cell surface (Figure 5B). This means that reversal of cellular motility causes reorientation of IgG-VSG movement. The redistribution of antibody-bound VSG toward the anterior pole of the cell was fast enough to clear the surface area around the flagellar pocket before significant amounts of IgG-VSG could be internalized as judged by the absence of detectable IgG in endosomes (Figure 5B). Taken together, these results suggest that the rapid redistribution of the immune complexes requires directional motility of the trypanosomes but is independent of endocytosis and the actin cytoskeleton.

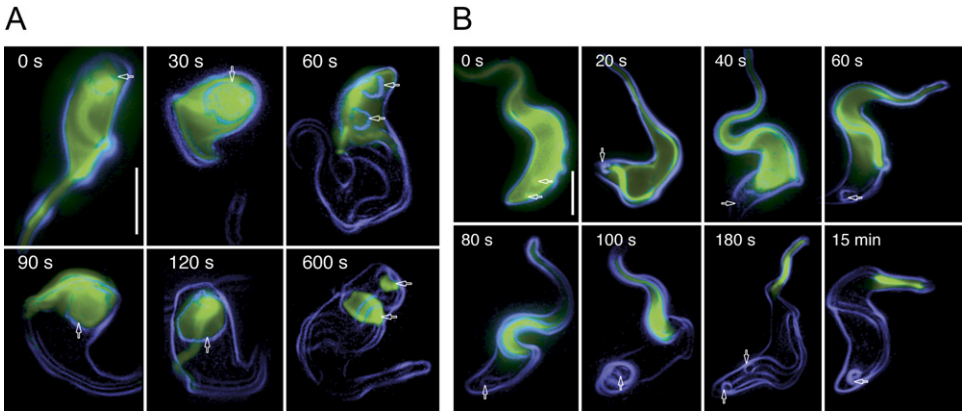

Figure 5. The Movement on the Cell Surface of IgG-VSG Is Independent of the Actin Cytoskeleton and Is Reversed in Backward-Swimming Cells

Following cell surface labeling with AMCA-sulfo-NHS (blue), trypanosomes were treated with 0.1 mg/ml VSG-specific IgG and incubated at a density of 10^8 cells/ml for 10 min on ice. Cells were incubated at 37°C for the times indicated, fixed, and permeabilized. Anti-VSG antibodies were detected with species-specific Alexa Fluor 488-conjugated second antibodies (green). Open arrows indicate the position of the flagellar pocket. Scale bar, 4 μm.

(A) Posterior accumulation of IgG-VSG does not require actin. Actin was downregulated by tetracycline-inducible RNAi (Garcia-Salcedo et al., 2004). After 10 hr of induction, cells reveal an enlarged flagellar pocket and arrested endocytosis; however, redistribution of IgG-VSG and uptake into the flagellar pocket are not impaired.

(B) The swimming direction determines the route of movement of IgG-VSG on the cell surface. Trypanosomes deprived of dynein arm intermediate chain (DNAI1) show backward motion (Branche et al., 2006) and reversed direction of IgG-VSG movement. RNAi against DNAI1 was induced for 10 hr.

The Size of Antibody-VSG Complexes Determines the Kinetics of Sorting

A physical explanation for the relationship between cell motility and the backward directional movement of IgG-VSG is the hydrodynamic drag force, which acts on the VSG-bound IgG during forward swimming of the trypanosome. If hydrodynamic forces were involved, the directional movement would be expected to depend on the size of the surface-bound ligand rather than its chemical characteristics. Therefore, the kinetics of surface clearance for a variety of ligands of different sizes was analyzed by flow cytometry (Table 1). Polyclonal or monoclonal IgGs were removed from the surface at similar rates ($t_{1/2}$ ~40 s), while smaller anti-VSG ligands like $F(ab')_2$ and Fab fragments were cleared at four to five times slower rates. Streptavidin was used as an alternative ligand after limited biotinylation of the cell surface and was cleared with similar kinetics as Fab fragments ($t_{1/2}$ ~170 s). In contrast, larger ligands like anti-VSG IgM (Figure 1A) or a bispecific antibody complex (TAC), an aggregate of two murine IgG_1 monoclonal antibodies held in a tetrameric array by two rat anti-IgG_1, were internalized two to three times faster than IgG-VSG. The fast surface clearance of IgG or IgM or TAC was accompanied by transient, posterior accumulation of VSG-ligand complexes. In contrast, posterior accumulation was not observed for the more slowly internalized ligands $F(ab')_2$, Fab, and streptavidin. Therefore, at a relatively low rate of backward redistribution, endocytosis is fast enough to prevent complex accumulation. Thus, these observations are consistent with the idea of a backward-directed drag force caused by the forward-swimming cell, while its magnitude is a function of ligand size.

A further prediction of this idea is that molecular crowding of surface-bound ligands will impair the overall rate of surface clearance, because abundant obstacles reduce the relative velocity of the surrounding liquid close to the surface. This was tested by increasing the amount of ligand bound to the cell surface from ~0.1% of the VSG dimers to about ~10%. The result was an increase in the half-time of clearance of IgG or IgM by a factor of 20 to 30 (Table S2). This observation implies that at high antibody concentrations clearance of immunoglobulin from the surface becomes inefficient.

Extrinsic Hydrodynamic Flow Forces Can Sort Proteins on Cell Surfaces

All the data pointed toward a hydrodynamic drag force-induced movement of antibody complexes on the cell surface of trypanosomes. But is such a mechanism physically possible? At first glance, this idea may seem odd, because it might be expected that continuum concepts like viscosity break down at the small dimensions of antibodies. However, the emerging view is that standard continuum dynamics is successful even at molecular scales (Bocquet and Barrat, 1996; Qian et al., 2003; Kadau et al., 2004; Priezjev et al., 2005). These recent studies may provide an explanation for earlier observations that an electro-osmotic flow of fluid suffices to directionally move proteins in the plane of the plasma membrane (McLaughlin and Poo, 1981; Levine et al., 1983; McCloskey et al., 1984).

A molecular model, schematically represented in Figure 6A, was used to estimate the strength of the drag force acting on a single IgG-VSG. Owing to hydrodynamic

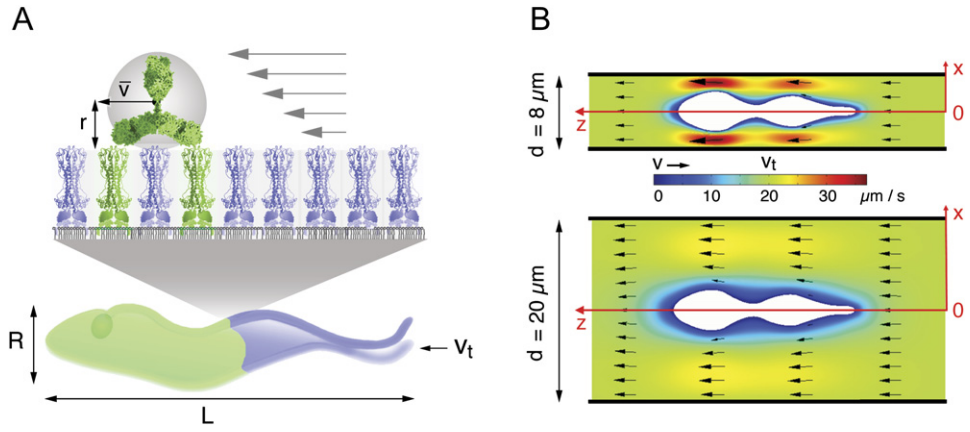

Figure 6. Hydrodynamic Flow Forces Can Drag VSG-IgG within the Trypanosome Surface Coat

(A) Schematic model of the proposed mechanism of VSG-IgG-complex movement. VSG and IgG are drawn to scale.

(B) Simulated velocity profiles for trypanosome-like bodies in capillaries of diameter of d = 8 μm or d = 20 μm.

flow, a spherical particle (IgG) of radius $r = 7.5$ nm is moving in parallel to the trypanosome surface coat with a mean velocity $\bar{v}$ in a bloodstream of viscosity $\eta = 0.03$ kg·m^{-1}s^{-1}. The velocity $\bar{v}$ of the IgG can be determined by assuming a linear velocity field and no-slip conditions (v = 0 at the coat surface). In this case we have $\bar{v} = r v_t / R$, where $v_t = 20$ μm/s (the mean swimming velocity of a trypanosome), r = 7.5 nm (the radius of the IgG ligand), and $R = 3$ μm (the mean diameter of a trypanosome). Therefore, the acting drag force is $F_D = -6\pi\eta r\bar{v} = -6\pi\eta r^2 v_t / R$. If there is a certain slip of the liquid at the trypanosome coat, $\bar{v}$, and thus F_D, will be larger by a factor (1 + b/r), where b, the so-called slip length, characterizes the strength of the slip (Richardson, 1973). At smooth surfaces, b may be easily of the same order of magnitude as r, or even larger (Cottin-Bizonne et al., 2005). If we further assume that the diffusion velocity is small as compared to $\bar{v}$, F_D can be assumed independent of the diffusive motion. It may then be described by means of a potential U, such that $F_D = -\,gradU$, or $U = -F_D h$, where h is the distance along the membrane surface in the direction of the flow. At a distance $h_0 = k_B T R / 6\pi\eta r^2 v_t \approx 20$ μm, where k_B is the Boltzmann constant and T is the absolute temperature, this energy equals the thermal energy $k_B T$ at 37°C. According to Boltzmann's law, the probability of finding a particle at this characteristic distance h_0 is 37% (1/*e*) that of finding it at zero distance. Since h_0 is in the order of magnitude of the trypanosome length L, the potential due to the drag force is in fact strong enough to generate the gradient in the distribution of IgG-VSG on the trypanosome surface, which was observed in the experiments. That such molecular drag forces may be quite substantial even close to a surface is well known (Bensimon et al., 1994, 1995) and is extensively used in research for aligning biomolecules (Chan et al., 2006; Dukkipati et al., 2006).

Smaller blood vessels, capillaries (diameter $d \approx 8$ μm) and venules ($d \approx 20$ μm), have diameters in the same order of magnitude as the size of a trypanosome. This similarity will influence the local flow fields in the vicinity of the trypanosome surfaces and therefore the time scale of the removal of IgG-VSG. The influence of these confining geometries on velocity fields was modeled by using numerical *f*inite element *m*ethod (FEM) simulations. The incompressible Navier-Stokes equation was solved in two dimensions with an axial symmetry (symmetry axis at x = 0) using about 30,000 elements (commercial software Femlab), and a stationary solution was obtained (low Reynolds numbers). The trypanosome was modeled by an axial symmetric body, and the flow was simulated by applying a constant velocity profile of $v_t = 20$ μm/s at $z = 0$ and a vanishing velocity at the trypanosome surface, $v_s = 0$. The simulated velocity profiles for trypanosome-like bodies in capillaries of diameters $d = 8$ μm and 20 μm are shown in Figure 6B. A decrease of the capillary diameter would lead to a strong increase of the velocity in the vicinity of the trypanosome surface. Owing to the increased local velocity, a higher drag force acts on the IgG-VSG, leading to faster removal of the antibodies.

DISCUSSION

Movement of Surface Proteins in Hydrodynamic Flow Fields

The protein-sorting mechanism proposed in this paper is based on a remarkable interplay between biochemical and structural peculiarities of the trypanosome and pure physical forces. The VSG coat (5×10^6 dimers per cell; about 10% of the cellular protein) provides a homogenous and densely packed platform from which antibodies can protrude into the surrounding medium. VSG dimers are anchored via glycosylphosphatidylinositol (GPI) residues to the plasma membrane (Figure 1A), do not interact with intracellular components such as the microtubular cytoskeleton, and are free to move in the plane of the membrane. In immobilized trypanosomes, VSG diffuses

laterally by random Brownian motion with a diffusion coefficient of 1×10^{-10} cm^2/s, so the mean travel distance in 60 min is 12 μm, less than the average length of a trypanosome (Bülow et al., 1988). This random movement cannot explain the observed rapid redistribution of the IgG-VSG complexes to the posterior pole (Figures 1 and 4), implying that some force must be applied to the IgG-VSG complexes. Both the abundance of VSG molecules and the surface attachment via GPI anchors means that the active movement of IgG-VSG complexes is unlikely to be mediated by interaction with some motor located inside the cell. The finding that the actin is not required supports this assumption (Figure 5A).

The flagellum is attached and runs along the body, propelling the cell in the direction away from the flagellar pocket. This causes the movement of immune complexes by hydrodynamic drag forces in the opposite direction. The flagellar pocket serves as a very effective sink for immune complex internalization. As shown in this study, the most rapid clearance occurred with IgM-VSG from stumpy trypanosomes because of ligand size and the accelerated rate of endocytosis (Table 1). This appears particularly important for survival of this nondividing stage, which is essential for transmission to the tsetse vector. Interestingly, infections by trypanosomes are characterized by the massive production of antibodies of the IgM class (Mansfield, 1994). We conclude that besides antigenic variation *T. brucei* has evolved a subtle defense strategy, in which directional cell motility and plasma membrane recycling function cooperatively in the removal of host antibodies from the cell surface. In an infected animal, antibody removal must be continuous, and clearance of trypanosomes can only occur when the host is producing VSG-specific immunoglobulins faster than the trypanosomes can degrade them. The proposed mechanism might be one reason why trypanosomes have been selected to maintain continuous high cellular motility (Broadhead et al., 2006). While this may be regarded as a unique adaptation of a parasite to its hostile environment, the flow-forced movement and sorting of proteins within the plasma membrane may well be a general organizing principle in other biological contexts, notably the vascular system of all animals with a pump-driven blood circulation.

Towing versus Rafting versus Sailing?

There are numerous reports on the directional redistribution of plasma membrane proteins in other cell types. Extensive crosslinking of cell surface proteins by antibodies or lectins in mammalian cells causes the passive patching of the molecules in the plane of the plasma membrane, followed by an energy-dependent coalescence at one end of the cell, a process called capping (Taylor et al., 1971; Rosen, 1979). Cap formation appears to be restricted to motile cells, such as fibroblasts, and requires an intact cytoskeleton (Bretscher, 1996). Capping has been explained by either a polarized actin cycle or a polarized endocytic cycle (for a review see Bretscher, 1996). Briefly, in the polarized actin cycle, microfilaments polymerizing at the leading edge push the cell forward. Backward-moving filamentous actin hooks up with patched membrane proteins on the cell surface, pulling the patches toward the posterior part of the cell, where actin depolymerizes and the cap forms. The alternative hypothesis, the polarized endocytic cycle, postulates that exocytosis at the leading edge locally extends the cell surface. Because endocytosis occurs randomly on the cell surface, a lipid flow is generated in the plasma membrane from the rear to the front end of the cell. This flow of plasma membrane transports patched surface proteins by default toward the back of the cell and the cap forms.

There are arguments in favor of either the actin cycle ("towing") or the endocytic cycle ("rafting"), but there is not a single case where either mechanism has been proven. The purely hydrodynamic sorting ("sailing") considered here depicts a very different scenario, as neither the actin nor the endocyctic cycle can account for the results. The redistribution of IgG-VSG is independent of both actin and endocytosis. In contrast, it critically depends on the size of the bound ligand, while patching and capping depends primarily on the valency of the ligands. Due to the dense packing of VSG in the surface coat, patches do not form. Viscosity or extracellular obstacles sustain directional swimming and IgG-VSG movement, an observation not expected to influence capping. Finally, reversal of the swimming direction reorients the movement of IgG-VSG. This can be explained neither by exo-/endocytic membrane flow, which in trypanosomes is highly localized, nor by the action of the cytoskeleton. We do not believe that our hydrodynamic model explains the capping on motile mammalian cells because their locomotion is generally too slow. But there may be fast-moving cells where the hydrodynamic flow influences the rate of capping, and experiments along the lines described in this paper may be revealing.

EXPERIMENTAL PROCEDURES

Trypanosomes

Throughout this study the monomorphic *T. brucei* variant MITat 1.2 (Cross and Manning, 1973) and the pleomorphic strain AnTat 1.1 (Delauw et al., 1985) were used. Pure populations of stumpy trypanosomes were obtained as described (Engstler and Boshart, 2004). The generation of transgenic cell lines for tetracycline-inducible RNA interference of clathrin heavy chain and FLA1 has been described earlier (Engstler et al., 2005). The clathrin heavy chain or the FLA1 protein was downregulated by a 12 or 8 hr incubation in the presence of 1 μg/ml tetracycline at 37°C, respectively. The actin and DNAI1 (dynein arm intermediate chain) RNAi cell lines were generated using published constructs (Garcia-Salcedo et al., 2004; Branche et al., 2006). Analysis of the transgenic trypanosomes was done 24 and 10 hr after induction with tetracycline, respectively.

Immunofluorescence Analysis

Bloodstream stage *Trypanosoma brucei* (strain MITat1.2) were cultivated in HMI-9 medium (Hirumi and Hirumi, 1989) containing 10% fetal calf serum, at 37°C in an atmosphere of 5% CO_2 in air. Cells were harvested at a density of 8×10^5 cells/ml by centrifugation at 1400 × g and 4°C for 10 min. After three washes with ice-cold trypanosome dilution buffer (TDB; 5 mM KCl, 80 mM NaCl, 1 mM $MgSO_4$, 20 mM

Na_2HPO_4, 2 mM NaH_2PO_4, 20 mM glucose [pH 7.4]), the cell density was adjusted to 1 × 10^8 cells/ml, and incubation with 1 mM AMCA-sulfo-NHS (Pierce, Rockford, IL) was performed for 10 min on ice in the dark. The reaction was stopped by the addition of 10 mM Tris-Cl (pH 8.5). After three washes with 2 ml of ice-cold TDB, 1% BSA, the cell suspension was adjusted to the density desired, treated with variant-specific anti-VSG antibodies, and washed. Aliquots of 50 μl were added to 450 μl of prewarmed (37°C) HMI-9 containing 50% fetal calf serum, and endocytosis was allowed for the times indicated, followed by two washes with ice-cold TDB. Throughout the procedure the cell viability was monitored by microscopy. Cells were fixed with 4% formaldehyde in PBS for 24 hr at 4°C. Permeabilization of trypanosomes was achieved by 15 min incubation in 500 μl of 0.1 M Na_2HPO_4/1 M glycine (pH 7.2), followed by 5 min incubation in 1 ml of 0.05 M Na_2HPO_4/0.5 M glycine/0.1% Triton X-100 (pH 7.2). As secondary reagents, specific Alexa Fluor-conjugated antibodies (1:2000, Molecular Probes) were diluted 1:1000 in PBS, 1% BSA.

Image Analysis

Image acquisition was performed with a motorized Zeiss Axiophot2 widefield microscope equipped with a Zeiss 63×/1.4 NA Oil DIC objective, a 1.6–2.5× optovar, and the CoolSnap HQ cooled (−30°C) CCD camera (Sony ICX285 interline, progressive-scan CCD; Photometrics). For acquisition of 3D images, a PIFOC objective z-stepper was driven by the piezo-amplifier E662 LVPZT (Physik Instrumente). The microscopic setup was integrated and controlled using the scripting features of the IPLab for Macintosh software (version 3.9, Scanalytics, Fairfax). For all images the exposure times were automatically adjusted to the desired maximum intensity signals, guaranteeing that no overexposure occurred. 3D images were acquired using the optimal sampling density derived from the optical setup, and the respective fluorophor (z-step size ≥ 50 × 100 nm). The point spread function of the microscope was measured using fluorescent 0.17 μm microspheres (PS-Speck Microscope Point Source Kit, Molecular Probes, Eugene, OR). Following image acquisition, the raw data were exported to the Huygens Essential software (version 2.9 for Mac OS X, Scientific Volume Imaging B.V., Hilversum), and digital deconvolution was performed using the "maximum likelihood estimation" (MLE) algorithm (>40 iterations). The restored image data set was visualized and analyzed with the Imaris software package, featuring the "Surpass" and "Coloc" modules (version 4.1.1 for Windows, Bitplane AG, Zurich).

Antibody Clearance Assays

Cells were surface labeled with AMCA-sulfo-NHS and incubated on ice for 10 min with specific antisera or immunoglobulins. AMCA-sulfo-NHS specifically stains the surface coat of live cells, while impaired or dead trypanosomes display a bright intracellular fluorescence. Following incubation at 37°C for varying times in HMI-9 medium containing 50% fetal calf serum, trypanosomes were chemically fixed with 4% formaldehyde. Cell-associated antibodies were detected with species-specific Alexa Fluor secondary antibodies (Molecular Probes). The time- and temperature-dependent localization of IgG was determined by semiautomatically scoring images of >300 cells for each time point. For visualization of endocytosed, VSG-bound antibodies, fixed trypanosomes were permeabilized with 0.1% Triton X-100.

For quantification of cell surface-bound antibodies, Alexa Fluor 488-conjugated secondary antibody was used, and fluorescence intensity was measured by flow cytometry. Clearance is expressed by the half-time of antibody decrease from the trypanosome cell surface. Data are means ± SEM (n = 4). For comparing the rates of surface clearance of IgG and IgM, trypanosomes were treated with varying amounts of immune serum containing rabbit anti-VSG IgG or carp anti-VSG IgM. Following incubation at 37°C for various times, surface-bound proteins were detected on fixed cells either directly or with fluorescently labeled secondary antibodies, and fluorescence quantification was done by flow cytometry.

Trypanosomes were surface biotinylated and incubated on ice with equal amounts of either affinity-purified anti-VSG IgG (0.2 mg/ml), the corresponding $F(ab')_2$ or Fab fragments, a mouse monoclonal anti-biotin antibody (Cy3-labeled), Alexa Fluor 594-conjugated streptavidin (Molecular Probes), or a tetrameric antibody complex (TAC; StemCell Technologies). The bispecific TAC consists of mouse monoclonal anti-biotin and anti-dextran IgG1 molecules linked by two rat monoclonal anti-mouse IgG1 molecules. An aliquot of the TAC-treated cells was incubated for another 10 min on ice with 2 mg/ml Cy3-conjugated dextran (M 10,000). The cells were warmed to 37°C and chemically fixed in intervals of 10 s with 4% formaldehyde, 0.05% glutaraldehyde. TACs were visualized with Cy3-conjugated dextran (M 10,000). For each time point microscopic images of >300 cells were recorded, and cell surface fluorescence was quantified by automated intensity segmentation (Grünfelder et al., 2002). Data are means ± SEM (n = 5).

Complement Lysis Assays

Cells were incubated for 10 min on ice in HMI-9 containing 50% fetal calf serum, in the presence of anti-VSG IgG, and washed. The temperature was raised to 37°C, and at the times indicated, 0.3 volumes of guinea pig serum (PromoCell) was added as a source of complement together with 1 mM AMCA-sulfo-NHS, and incubation was continued at 37°C for 25 min, followed by washing and chemical fixation. For each time point microscopic images of >300 cells were analyzed by automated fluorescence threshold segmentation. Dead cells were detected by strong intracellular AMCA fluorescence, while viable trypanosomes revealed characteristic cell surface fluorescence only. Values are means ± SEM (n = 4).

Purification and Quantification of Immunoglobulins

IgG-containing rabbit anti-VSG serum was loaded on Protein G cross-linked 4% beaded agarose fast flow, equilibrated in 20 mM sodium phosphate buffer (pH 7.0). Following washing with 4 column volumes of 20 mM sodium phosphate buffer (pH 7.0), elution of IgG was done at slow flow rates with 2 column volumes of 100 mM glycine-Cl (pH 2.7). The IgG-containing eluate was adjusted to pH 7 with 0.1 N NaOH. The yield of anti-VSG IgG was determined by quantitative western blotting using purified rabbit IgG (Jackson ImmunoResearch) as standard. The quantity of antibody bound to live trypanosomes was estimated by incubating cells with varying amounts of VSG-specific IgG (0–2 mg). Following centrifugation the IgG concentration in the supernatant was determined by quantitative western blotting. Trypanosomes expressing a different VSG variant served as specificity control. The number of bound IgG molecules was calculated assuming that a single trypanosome displays 10^7 VSG molecules on the cell surface.

Anti-VSG IgM was produced in carp. The fish (R3 × R8) were an offspring of a cross between the Hungarian strain R8 and the Polish strain R3. Eight carp weighing between 650 and 950 g were immunized with 400 μg each of purified VSG in incomplete Freund's adjuvant. Four animals each were immunized intramuscularly and intraperitoneally. The second immunization was after 6 weeks. The first bleeding was after 9 weeks, and the second bleeding was 2 weeks later. The specificity of the IgM-containing carp sera was tested by immunofluorescence analysis using the mouse monoclonal anti-carp IgM WCI-12 diluted 1:500 as second antibody and the respective preimmune sera as control. Anti-VSG IgM was purified using the ImmunoPure IgM Purification Kit (Pierce) following the instructions provided by the manufacturer. The yield and purity of IgM were determined by quantitative western blotting.

Supplemental Data

Supplemental Data include three figures and two tables and can be found with this article online at http://www.cell.com/cgi/content/full/131/3/505/DC1/.

ACKNOWLEDGMENTS

This work was supported by the Deutsche Forschungsgemeinschaft (grants EN305/2-1, EN305/2-2, EN305/4-1, and PF375/5-1), the Max-Planck-Gesellschaft, and the Fonds der Chemischen Industrie. We are grateful to F. Weise (NMI Tübingen) for help in initial experiments and to M. Carrington (University of Cambridge) for critical reading of the manuscript and momentous discussion. We are indebted to J. Donelson (University of Iowa) for the gift of the p2T7-FLAI plasmid, D. Nolan (Trinity College, Dublin) for the pZJM-actin construct, and P. Bastin (Institute Pasteur) for the pZJM-DNAI1 plasmid. We thank G.A.M. Cross (The Rockefeller University), K. Gull (University of Oxford), M. Carrington, and M.C. Field (University of Cambridge) for providing antibodies.

Received: March 15, 2007
Revised: June 19, 2007
Accepted: August 27, 2007
Published: November 1, 2007

REFERENCES

Allen, C.L., Goulding, D., and Field, M.C. (2003). Clathrin-mediated endocytosis is essential in *Trypanosoma brucei*. EMBO J. *22*, 4991–5002.

Balber, A.E., Bangs, J.E., Jones, S.M., and Poia, R.L. (1979). Inactivation or elimination of potentially trypanolytic, complement-activating immune complexes by pathogenic trypanosomes. Infect. Immun. *24*, 617–627.

Barry, J.D. (1979). Capping of variable antigen on *Trypanosoma brucei*, and its immunological and biological significance. J. Cell Sci. *37*, 287–302.

Barry, J.D., and McCulloch, R. (2001). Antigenic variation in trypanosomes: Enhanced phenotypic variation in a eukaryotic parasite. Adv. Parasitol. *49*, 1–70.

Bensimon, A., Simon, A.J., Chiffaudel, A., Croquette, V., Heslot, F., and Bensimon, D. (1994). Alignment and sensitive detection of DNA by a moving interface. Science *265*, 2096–2098.

Bensimon, D., Simon, A.J., Croquette, V., and Bensimon, A. (1995). Stretching DNA with a receding meniscus: Experiments and models. Phys. Rev. Lett. *74*, 4754–4757.

Bocquet, L., and Barrat, J.L. (1996). Hydrodynamic properties of confined fluids. J. Phys.: Cond. Matter. *8*, 9297–9300.

Branche, C., Kohl, L., Toutirais, G., Buisson, J., Cosson, J., and Bastin, P. (2006). Conserved and specific functions of axoneme components in trypanosome motility. J. Cell Sci. *119*, 3443–3455.

Bretscher, M.S. (1996). Moving membrane up to the front of migrating cells. Cell *85*, 465–467.

Broadhead, R., Dawe, H.R., Farr, H., Griffiths, S., Hart, S.R., Portman, N., Shaw, M.K., Ginger, M.L., Gaskell, S.J., McKean, P.G., and Gull, K. (2006). Flagellar motility is required for the viability of the bloodstream trypanosome. Nature *440*, 224–227.

Bülow, R., Overath, P., and Davoust, J. (1988). Rapid lateral diffusion of the variant surface glycoprotein in the coat of *Trypanosoma brucei*. Biochemistry *27*, 2384–2388.

Chan, T.-F., Ha, C., Phong, A., Cai, D., Wan, E., Leung, L., Kwok, P.Y., and Xiao, M. (2006). A simple DNA stretching method for fluorescence imaging of single DNA molecules. Nucleic Acids Res. *34*, e113.

Cottin-Bizonne, C., Cross, B., Steinberger, A., and Charlaix, E. (2005). Boundary slip on smooth hydrophobic surfaces: Intrinsic effects and possible artifacts. Phys. Rev. Lett. *94*, 056102.

Cross, G.A.M. (1996). Antigenic variation in trypanosomes: Secrets surface slowly. Bioessays *1*, 283–291.

Cross, G.A.M., and Manning, J.C. (1973). Cultivation of *Trypanosoma brucei* spp. in semi-defined and defined media. Parasitology *67*, 315–331.

Delauw, M.-F., Pays, E., Steinert, M., Aerts, D., Van Meirvenne, N., and Le Ray, D. (1985). Inactivation and reactivation of a variant-specific antigen gene in cyclically transmitted *Trypanosoma brucei*. EMBO J. *4*, 989–993.

Donelson, J.E., Hill, K.E., and El-Sayed, N.M.A. (1998). Multiple mechanisms of immune evasion by African trypanosomes. Mol. Biochem. Parasitol. *91*, 51–66.

Dukkipati, V.R., Kim, J.H., Pang, S.W., and Larson, R.G. (2006). Protein-assisted stretching and immobilization of DNA molecules in a microchannel. Nano Lett. *6*, 2499–2504.

Engstler, M., and Boshart, M. (2004). Cold shock and regulation of surface protein trafficking convey sensitization to inducers of stage differentiation in *Trypanosoma brucei*. Genes Dev. *18*, 2798–2811.

Engstler, M., Thilo, L., Weise, F., Grünfelder, C.G., Schwarz, H., Boshart, M., and Overath, P. (2004). Kinetics of endocytosis and recycling of the GPI-anchored variant surface glycoprotein in *Trypanosoma brucei*. J. Cell Sci. *117*, 1105–1115.

Engstler, M., Weise, F., Bopp, K., Grünfelder, C.G., Günzel, M., Heddergott, N., and Overath, P. (2005). The membrane-bound histidine acid phosphatase TbMBAP1 is essential for endocytosis and membrane recycling in *Trypanosoma brucei*. J. Cell Sci. *118*, 2105–2118.

Fache, S., Dalous, J., Engelund, M., Hansen, C., Chamaraux, F., Fourcade, B., Satre, M., Devreotes, P., and Bruckert, F. (2005). Calcium mobilization stimulates *Dictyostelium discoideum* shear-force-induced cell motility. J. Cell Sci. *118*, 3445–3457.

Garcia-Salcedo, J.A., Perez-Morga, D., Gijon, P., Dilbeck, V., Pays, E., and Nolan, D.P. (2004). A differential role for actin during the life cycle of *Trypanosoma brucei*. EMBO J. *25*, 780–789.

Grünfelder, C.G., Engstler, M., Weise, F., Schwarz, H., Stierhof, Y.-D., Boshart, M., and Overath, P. (2002). Accumulation of a GPI-anchored protein at the cell surface requires sorting at multiple intracellular levels. Traffic *3*, 547–559.

Hirumi, H., and Hirumi, K. (1989). Continuous cultivation of *Trypanosoma brucei* blood stream forms in a medium containing a low concentration of serum protein without feeder cell layers. J. Parasitol. *75*, 985–989.

Kadau, K., Germann, T.C., Hadjiconstantinou, N.G., Lomdahl, P.S., Dimonte, G., Holian, B.L., and Alder, B.J. (2004). Nanohydrodynamics simulations: An atomistic view of the Rayleigh-Taylor instability. Proc. Natl. Acad. Sci. USA *101*, 5851–5855.

LaCount, D.J., Barrett, B., and Donelson, J.E. (2002). *Trypanosoma brucei* FLA1 is required for flagellum attachment and cytokinesis. J. Biol. Chem. *277*, 17580–17588.

Levine, S., Levine, M., Sharp, K.A., and Brooks, D.E. (1983). Theory of the electrokinetic behavior of human erythrocytes. Biophys. J. *42*, 127–135.

Mansfield, J.M. (1994). T-cell responses to the trypanosome variant surface glycoprotein: A new paradigm? Parasitol. Today *10*, 267–270.

McCloskey, M.A., Liu, Z.Y., and Poo, M.M. (1984). Lateral electromigration and diffusion of Fc epsilon receptors on rat basophilic leukemia cells: Effects of IgE binding. J. Cell Biol. *99*, 778–787.

McLaughlin, S., and Poo, M.M. (1981). The role of electro-osmosis in the electric-field-induced movement of charged macromolecules on the surfaces of cells. Biophys. J. *34*, 85–93.

McLintock, L.M.L., Turner, C.M.R., and Vickerman, K. (1993). Comparison of the effects of immune killing mechanisms on *Trypanosoma brucei* parasites of slender and stumpy morphology. Parasite Immunol. *15*, 475–480.

O'Beirne, C., Lowry, C.M., and Voorheis, H.P. (1998). Both IgM and IgG anti-VSG antibodies initiate a cycle of aggregation of bloodstream

forms of *Trypanosoma brucei* without damage to the parasite. Mol. Biochem. Parasitol. *91*, 165–193.

Overath, P., and Engstler, M. (2004). Endocytosis, membrane recycling and sorting of GPI-anchored proteins: *Trypanosoma brucei* as a model system. Mol. Microbiol. *53*, 735–744.

Pal, A., Hall, B.S., Jeffries, T.R., and Field, M.C. (2003). Rab5 and Rab11 mediate transferrin and anti-variant surface glycoprotein antibody recycling in *Trypanosoma brucei*. Biochem. J. *374*, 443–451.

Phan, U.T., Waldron, T.T., and Springer, T.A. (2006). Remodeling of the lectin-EGF-like domain interface in P- and L-selectin increases adhesiveness and shear resistance under hydrodynamic force. Nat. Immunol. *8*, 883–889.

Priezjev, N.V., Darhuber, A.A., and Troian, S.M. (2005). Slip behavior in liquid films on surfaces of patterned wettability: Comparison between continuum and molecular dynamics simulations. Phys. Rev. E Stat. Nonlin. Soft Matter Phys. *71*, 041608/1–041608/11.

Qian, T., Wang, X.-P., and Sheng, P. (2003). Molecular scale contact line hydrodynamics of immiscible flows. Phys. Rev. E Stat. Nonlin. Soft Matter Phys. *68*, 016306/1–016306/15.

Richardson, S. (1973). On the no-slip boundary condition. J. Fluid Mech. *59*, 707–719.

Rosen, R. (1979). Patching and capping of cell membrane receptors as examples of morphogenetic movement. J. Theor. Biol. *80*, 149–153.

Russo, D.C.W., Grab, D.J., Lonsdale-Eccles, J.D., Shaw, M.K., and Williams, D.J.L. (1993). Directional movement of variable surface glycoprotein-antibody complexes in *Trypanosoma brucei*. Eur. J. Biochem. *62*, 432–441.

Singer, S.J., and Nicolson, G.L. (1972). The fluid mosaic model of the structure of cell membranes. Science *175*, 720–731.

Stevens, D.R., and Moulton, J.E. (1978). Ultrastructural and immunological aspects of the phagocytosis of *Trypanosoma brucei* by mouse peritoneal macrophages. Infect. Immun. *19*, 972–982.

Taylor, R.B., Duffus, W.P.H., Raff, M.C., and de Petris, S. (1971). Redistribution and pinocytosis of lymphocyte surface immunoglobulin molecules induced by anti-immunoglobulin antibody. Nat. New Biol. *233*, 225–229.

Tzima, E. (2006). Role of small GTPases in endothelial cytoskeletal dynamics and the shear stress response. Circ. Res. *98*, 176–185.

Webster, P., Russo, D.C.W., and Black, S.J. (1990). The interaction of *Trypanosoma brucei* with antibodies to variant surface glycoproteins. J. Cell Sci. *96*, 249–255.